

Supramolecular Polymerization of DNA Double-Crossover-Like Motifs in Various Dimensions

Cuizheng Zhang[#], Dake Mao[#], Victoria E. Paluzzi, and Chengde Mao^{*}

Department of Chemistry, Purdue University, West Lafayette, IN 47906, USA

[#]These authors contribute equally

Abstract Double-crossover-like (DXL) molecules are a series of DNA motifs containing two strands with identical or different sequences. These homo- or hetero-dimers can further polymerize into bulk structures through specific hydrogen bonding between sticky ends. DXL molecules have high designability, predictivity and sequence robustness; and their supramolecular polymerization products would easily achieve controllable morphology. In addition, among all available DNA nanomotifs, DXL molecules are small in size so that the cost of DXL-based nanostructures is low. These properties together make DXL-based nanostructures good candidates for patterning, templating, information and matter storage, etc. Herein, we will discuss DXL motifs in terms of the detailed molecular design, and their supramolecular polymerization in various dimensions, and related applications.

Keywords DNA nanotechnology; Palindromic sequence; Helical twisting; Supramolecular polymerization; Controllable morphology

Citation: Zhang, C.; Mao, D.; Paluzzi, V. E.; Mao, C. Supramolecular Polymerization of DNA Double-Crossover-Like Motifs in Various Dimensions. *Chinese J. Polym. Sci.* ???, ???, ???.

INTRODUCTION

Supramolecular polymerization relies on non-covalent bonds to associate individual monomers together.¹⁻³ It offers many unique properties, particularly for processing of polymeric materials and has been extensively studied with a wide range of molecular systems.⁴⁻⁶ This manuscript reviews the supramolecular polymerization of a specific type of DNA monomer: double crossover-like (DXL) motif in various dimensions. DNA is best known as the carrier for genetic information. DNA also provides an excellent molecular system to study supramolecular polymerization for two reasons: i) highly predictable Watson-Crick base pairing via specific hydrogen bonding (H-bonding) between A-T and G-C, respectively; ii) well-established secondary structure, double-helix structure. These two properties together lead to the development of DNA-based nanomaterials.⁷⁻⁹ Generally, small DNA molecules (molecular weight, MW, $< 3 \times 10^4$ g/mol when less than 100 nucleotides) with well-designed sequences associate with each other via H-bonding into small motifs, which further associate with each other into final large polymers (e.g. MW $\sim 10^{16}$ g/mol for a DNA crystal with the size around 100 $\mu\text{m} \times 100 \mu\text{m} \times 100 \mu\text{m}$).

A DXL motif contains two DNA strands, identical or different (Fig. 1).¹⁰ Based on the sequence design, the two DNA strands can associate with each other into two double helices (duplexes) that are connected via two strand crossovers. The two duplex domains are both $N + \frac{1}{2}$ helical turns long where N could be zero. In this geometry, the DNA strands can crossover from one duplex domain to the other. In addition, the DXL has four free, single-stranded ends (Fig. 1a, top view), which are called sticky ends because base pairing between those sticky ends would allow individual DXL motifs to stick/associate with each other into polymers. If we view this DXL motif globally, it is also a left-handed, double helix which all base pair planes are parallel to the helical axis.¹¹

The DXL motif is a flat molecule, and the two duplex domains consists of a plane (Fig. 1a, left view). When two DXL motifs associate with each other via sticky-end cohesion, the two molecules will rotate around the associating duplex relative to each other. Each duplex turn consists of 10.5 base pairs (bps), so each base pair rotates around the helical axis by $360^\circ / 10.5 = 34.3^\circ$ right-handedly. Thus, the rotation angle can be calculated according to the repeating distance of the DXL motif (Fig. 1b). Depending on the value of the rotational angle, DXL motifs will polymerize in one (1D)-, or two (2D)-, or three-dimensions (3D), leading to a range of controllable morphologies for patterning, templating, and information and matter storage, etc. In addition, the DXL molecule consists of only one or two unique DNA sequences. Such a minimal number of component strands helps to avoid

* Corresponding authors: E-mail mao@purdue.edu (Mao C.)
Invited Review
Received ???; Accepted ???; Published online ???

complicated stoichiometry and dramatically decreases the cost.

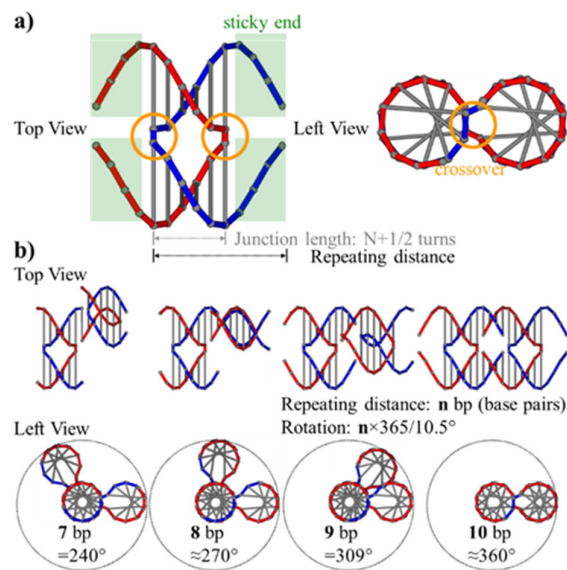


Figure 1 The structure of the DXL motif and the rotational angle between two interacting DXL motifs. (a) A DXL motif consists of two either identical or different ssDNA. Two crossovers connect two duplexes and the distance between them should be $N+1/2$ helical turns where N is zero or any positive integral number. Four sticky ends flank the two central helical domains and contribute to the repeating distance which is the sum of the helical domain length and the length of sticky ends. (b) According to the repeating distance, the rotational angle between two interacting DXL motifs could be rationally designed and predicted.

1D POLYMERIZATION

We have studied 1D polymerization with two families of DXL motifs of different sizes.^{12,13} The central duplex domains are either 1.5 or 0.5-turn-long (16 or 6 bps) (Fig. 2). The ssDNA could initially hybridize to a structural monomer by the palindromic domains. As explained in Fig. 1b, only when the overall repeating distance is an integral number of helical turns (Figs. 2a2 and 2b2), final supramolecular polymerization products will be 1D linear chains via sticky ends. So, for the DXL motif with a one and half-turn-long central helical domain, the length of its sticky ends should be 4-6 nucleotides to make the repeating length close to the integral turns. Then one motif would rotate fully 360° to pair with the adjacent motif through sticky ends on both the 5' and 3' ends at the same time to form a 1D chain (Fig. 2a2). Moreover, the supercoil could be introduced on the center helical domain to bend these straight chains (Figs. 2a3-2a5). Even though the optimized distance between two crossovers inside one DXL monomer is an odd number of half-turns, DXL monomers still could form with extra under-winding or over-winding, which could twist the monomer and further polymerize into curved and helical chains with fixed curvature, such as waves or circle morphology. Under the characterization of atomic force microscope (AFM), the degree of winding increased when the difference between

twisted and optimized DXL increased according to the decreased radius of the final helical structures (Figs. 2a3-2a5).

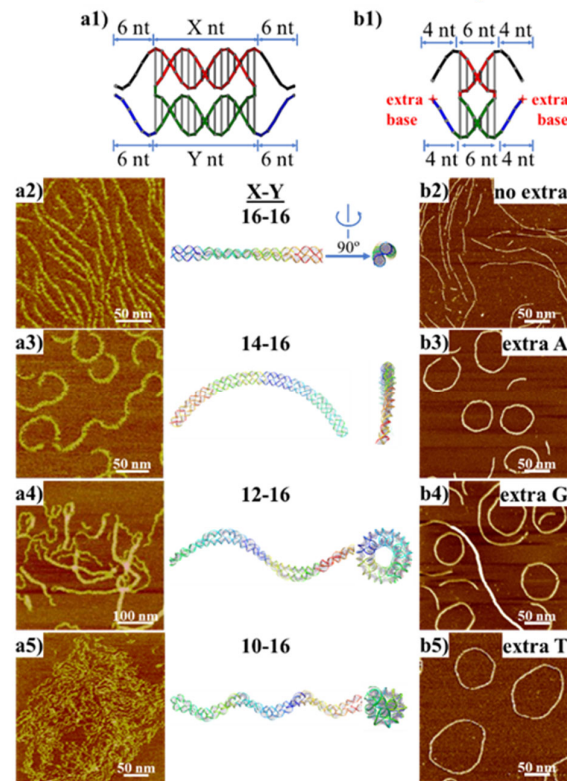


Figure 2 Supramolecular homo-polymerization of DXL motifs into straight or curved chains. (a) Two copies of a ssDNA consisting of four palindromes (colored differently) homodimerize into a DXL monomer, then further polymerize into straight or curved chains based on the supercoil of the center helical domains. All interactions rely on DNA hybridization of sticky ends. The arrows indicate the positions of 3' ends. For polymers assembled from each DXL monomer, an AFM image is presented to the left and two different views of CanDo predicted structures are presented to the right. Reproduced/Adapted from 10.1002/marc.202100217 with permission from Macromolecular Rapid Communications. (b) Two copies of a ssDNA consisting of four palindromes (colored differently) homodimerize into a DXL monomer, then further polymerize into straight or curved chains based on stacking of the extruding unpaired base outside the sticky ends into the helical domains. All interactions rely on DNA hybridization of sticky ends. The arrows indicate the positions of 3' ends. For polymers assembled from each DXL monomer, an AFM image is presented. Reproduced/Adapted from 10.1039/D2NR05404C with permission from The Royal Society of Chemistry.

For the DXL motif with half-turn-long central helical domain, the length of its sticky ends should be either 4 or 5 nucleotides. Then, the condition of Fig. 2b2 would be the same as the Fig. 1b. Furthermore, the bending of this polymer could be tuned by introducing an extra chemical group (Z) at the 3' end. Even though the length of the center helical domains is optimized, when the Z inserts into DNA duplexes by aromatic stacking, it will cause the length of the 3' end helices to be longer than that of the 5' end helices, which makes the final products curved (Figs. 2b3-2b5). Moreover,

the stacking in and flipping out of the extra base Z is under dynamic equilibrium, which enables flexible change of the curvature.

2D POLYMERIZATION

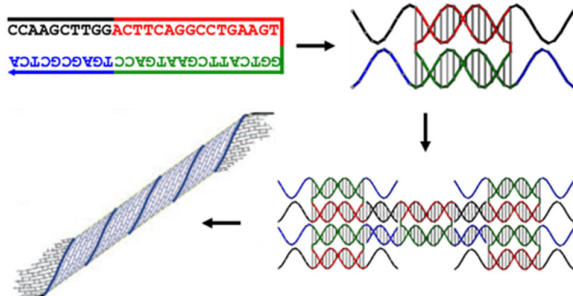


Figure 3 Two copies of ssDNA consisting of four palindromes (colored differently) that homodimerize into a DXL monomer, then further polymerize into 2D arrays or even further fold into nanotubes. All interactions rely on DNA hybridization of sticky ends. The arrows indicate the positions of 3' ends. Reproduced/Adapted from 10.1002/anie.200504022 with permission from Angewandte Chemie International edition.

The DXL DNA polymerization provides a novel approach to assemble DNA 2D nanosheet and nanotube.¹⁴⁻¹⁸ Compared with the 1D structures from Fig. 2a2, 2D products could be easily achieved by elongating the length of the sticky ends (Fig. 3).^{10,19,20} Now the length of four palindromes is 10, 16, 16 and 10 nt thus the overall repeating distance is an odd number of half-turns (16+10=26 bp, 5 half-turns). According to the helical feather of B-type DNA duplex, when two DXL molecules interact with each other through sticky ends hybridization, one molecule needs to flip roughly 180° ($360^\circ/10.5 \times 26 = 891^\circ = 720^\circ + 171^\circ$) compared with the other, and such flipping happens for all adjacent DXL monomers to further polymerize into the final 2D arrays. Because many nicks exist at the crossover points, the 2D lattices are not stiff and could fold into nanotubes.

The assembly process and thermodynamic property of the DXL nanotube was also studied later. F. C. Simmel et al. focused on the melting process.²¹ They demonstrated that a folded nanotube has extra thermodynamic stability compared with an open 2D sheet. So, this is the motivation force for forming DXL nanotubes instead of 2D sheets when annealing all ssDNAs directly in solution. Another study revealed the DXL nanotube assembly is related with two competing and temperature dependent parameters: (i) the conformation arrangement rate of DNA strands; and (ii) the growing rate of new strands on the nuclei.²² For example, under high DNA concentrations or strong binding force, the growing rate will be faster but more defects will be introduced into the final structure at the same time.

3D POLYMERIZATION

DNA 3D crystals could be built with designable symmetry based on the same strategy if DXL molecules are aligned periodically at different planes on purpose (Fig. 4).²³ By changing the length of the sticky ends to some certain numbers compared with the 1D structures (Fig. 2b1), the

rotational axis could be set to 120° (3-fold rotational axis, 7-base-pair-long repeating distance: $360/10.5 \times 7 = 240^\circ$, Figs. 1b and 4a) or 90° (4-fold rotational axis, 8-base-pair-long repeating distance: $360/10.5 \times 8 \approx 270^\circ$, Figs. 1b and 4f).

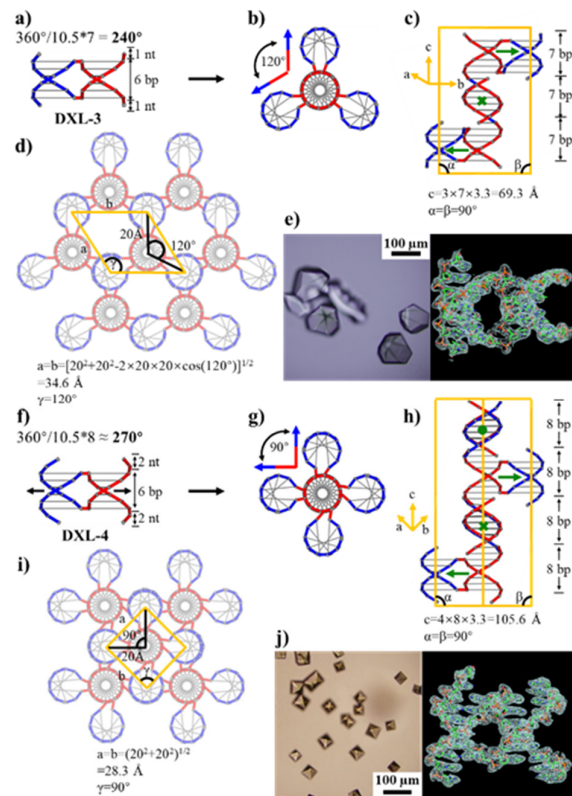


Figure 4 Supramolecular homo-polymerization of DXL into 3D crystals. (a) The DXL-3 molecule which is a hetero-dimer of two different 14-nt-long strands. The pair of red sticky ends are complementary to each other; the same to the pair of blue sticky ends. Three motifs associated along one duplex via sticky-end cohesion viewed (b) along and (c) perpendicular to the duplex. A 3₂-screw axis exists along the pseudo-continuous duplex. DNA crystals in the P3₂ space group with predictable unit cell parameters viewed (d) along and (e) perpendicular to the duplex. (e) The optical image of the final polymerized DNA 3D crystals. The solved structure is next to the crystal image with a 2Fo-Fc electron density map contoured at 1.5 σ within 2.6 Å resolution (PDB ID: 8EPB). (f) The DXL-4 molecule, which is a homodimer of two identical 16-nt-long strands. The pair of red sticky ends are complementary to each other; the same to the pair of blue sticky ends. Two horizontal arrows indicate the two-fold rotational axis according to the DNA backbone. Four motifs associated along one duplex via sticky-end cohesion viewed (g) along and (h) perpendicular to the duplex. A 4₃-screw axis exists along the pseudo-continuous duplex. DNA crystals in the P4₃22 space group with predictable unit cell parameters viewed (g) along and (i) perpendicular to the duplex. (j) The optical image of the final polymerized DNA 3D crystals. The solved structure is next to the crystal image with a 2Fo-Fc electron density map contoured at 1.5 σ within 2.2 Å resolution (PDB ID: 8EPG). Reprinted (adapted) with permission from {J. Am. Chem. Soc. 2023, 145, 8, 4853–4859}. Copyright {2023} American Chemical Society.

When two DXL-3 motifs associate through sticky-end cohesion at either the 5' or 3' ends, one motif, relative to the other, translates along the interacting duplex by 7 bp and rotates right-handedly around the interacting duplex by 240°. Every three motifs will complete two full turns because the repeating distance along the duplex is $3 \times 7 = 21$ bp. Thus, there is a 3_2 -screw axis along the duplex. When viewing along the interacting duplex, the other helical domains of the motifs are arranged around the interacting duplex and separated away from each other by 120° (Figs. 4b and 4c). The same will happen to all other duplexes so all DNA duplexes are in parallel to each other in a triangular fashion in the final crystal (Fig. 4d). From this model, we can calculate the unit cell parameters based on the parameters of an ideal B-type DNA duplex (assuming the duplex diameter is 20 Å; the rise is 3.3 Å per bp; and there is no space between adjacent duplexes), $a = b = 34.6$ Å and $c = 69.3$ Å (Figs. 4c and 4d) and we can predict that the final crystal will fall into the $P3_2$ space group with triangle-like shapes (Fig. 4e).

A similar prediction could be made on DXL-4 motifs. Every four motifs will complete three full turns ($4 \times 8 = 32$ bp) and there is a $P4_3$ -screw axis along the duplex. When viewing along the interacting duplex, the other helical domains of the motifs are arranged around the interacting duplex and separated away from each other by 270° right-handedly (Figs. 4g and 4h). The same will happen to all other duplexes so all DNA duplexes are in parallel to each other in a tetragonal fashion in the final crystal (Fig. 4i). From this model, $a = b = 28.3$ Å and $c = 105.6$ Å (Figs. 4h and 4i) and we can predict that the final crystal will fall into the $P4_3$ space group for two-stranded hetero-dimerized asymmetric designs or the $P4_322$ space group for one-stranded homo-dimerized symmetric designs with square-like shapes (Fig. 4j). Beyond the consistency between the designed structures and experimental results, this series of crystals can reach the highest resolution (2.2 Å) among all the rationally designed DNA crystals so far (Figs. 4e and 4j).

BIOMEDICAL APPLICATIONS OF DXL POLYMERIZATION

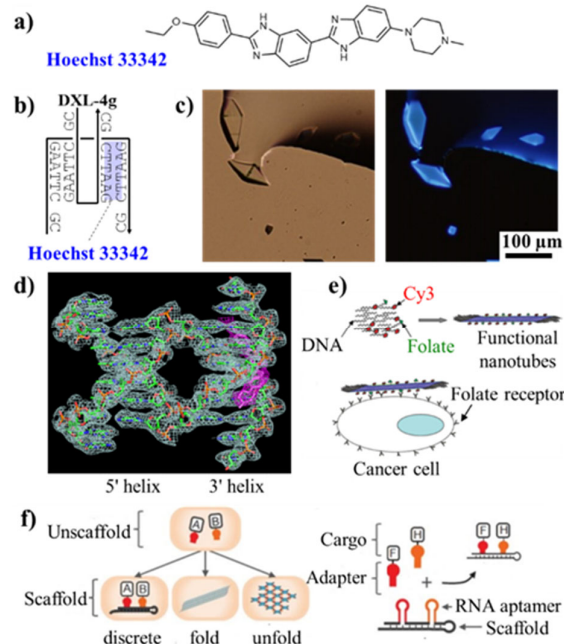


Figure 5 DXL supramolecular polymerized products used in biomedical research related applications. (a) Hoechst 33342 structure. (b) DXL/Hoechst complex. (c) Bright field (left) and fluorescence (right) images of DNA-Hoechst 33342 complex crystals. (d) The solved crystal structure of DXL/Hoechst 33342 complex with 2Fo-Fc electron density map contoured at 1.0 σ for DXL and 0.5 σ for Hoechst 33342 within 2.55 Å resolution (PDB ID: 8F42). Hoechst 33342 in purple. Reprinted (adapted) with permission from *{J. Am. Chem. Soc. 2023, 145, 8, 4853–4859}*. Copyright {2023} American Chemical Society. (e) DXL nanotube as a cell delivery platform. Reprinted (adapted) with permission from *{Biomacromolecules 2008, 9, 11, 3039–3043}*. Copyright {2008} American Chemical Society. (f) In vivo RNA DXL structure formation and engineering with hydrogen production in bacteria. Reproduced/Adapted from 10.1126/science.1206938 with permission from Science.

DXL polymerization has been applied in biomedical research, such as DNA-guest molecule interaction studies, cell delivery and bacteria protein engineering. Since 1982, the holy grail of DNA crystal engineering is to co-crystallize DNA and guest molecules in the 3D space to either determine the guest molecule structures or study their interactions.^{24,25} Such a study has not been developed for at least twenty years due to the modest resolution of previously designed DNA crystals. The high resolution achieved in DXL 3D crystals enables such applications (Figs. 5a-5d). Hoechst 33342 was used as the model molecule (Fig. 5a) which has blue fluorescence and can bind to the minor groove of DNA duplex, preferably at A/T-rich sequences (5'-GAATTC-3').²³ The DXL molecule could co-crystallized with Hoechst 33342 without dramatically changing the pure DNA crystal structure, and the interaction between DNA and dye was demonstrated by fluorescence of the entire crystal. (Figs. 5b and 5c). The crystals diffracted well so that the Hoechst 33342

molecule could be unambiguously modeled into the electron density map under the resolution of 2.55 Å (PDB ID: 8F42). The molecule bound to the minor groove of the 3' helix at the sequence of 5'-GAATTC-3' as the predicted (Fig. 5d) and the binding interaction between the DNA duplex and Hoechst 33342 in this study matched well with the previously reported crystal structure of DNA duplex-Hoechst 33342 (PDB ID: 129D).

Besides, self-assembly DNA nanostructures are widely applied in cell delivery and engineering. The DXL DNA polymerization provides a robust and simplified approach for synthesizing and constructing the functional DNA nanotubes and 2D nanosheets.²⁶⁻²⁸ The one-stranded homodimerized symmetric design with folate acid and Cy3 dye has been assembled into tubes with micrometer length and applied in cancer cell delivery (Fig. 5e).²⁹ With folate acid, the nanotubes could target the cancer cell and efficiently enhance the cell uptake, while obvious toxicity was not observed. Moreover, such DXL nanotube designs could facilitate in vivo applications by producing the oligonucleotide through transcription machinery since they have the smallest number of strands. The DXL RNA nanostructure has been transcribed and assembled in bacteria based on the similar design principle and further used as scaffolds for the spatial organization of [FeFe]-hydrogenase and ferredoxin (Fig. 5f).³⁰ By controlling the spatial arrangement to organize the enzymatic pathways, the RNA scaffolds could optimize hydrogen production, demonstrating that nucleic acid assemblies are able to engineer the biological pathways of bacteria metabolism.

DXL POLYMERIZATION IN NOVEL MATERIALS

Recently, plenty of new materials and material fabrication studies have been reported based on versatile DXL DNA supramolecular polymerization. A hydrogel was constructed by DXL linear polymers with its homo-polymerization property and kinetic interlocking (Fig. 6a).³¹ With the help of the rigid unit in the DXL monomer, the polymer was endowed with high stability. By introducing the extruding i-motif domain on the DXL monomer, such a homopolymer could be crosslinked and form a pH-responsive hydrogel. Due to the structural rigidity and strong intramolecular interactions in the DNA monomer, the hydrogel exhibited comparable mechanical strength and low gelation concentration with extreme high molecular weight.

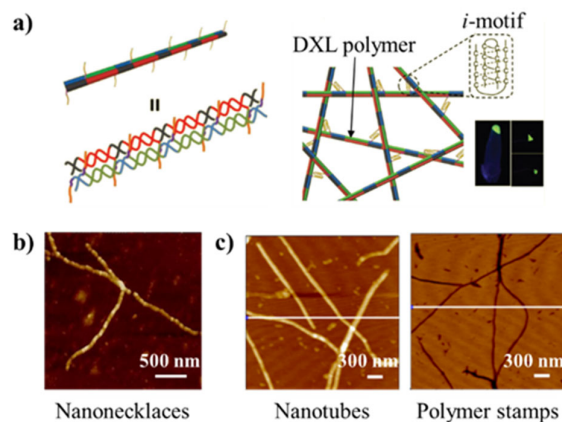


Figure 6 DXL supramolecular polymerized products used in material science related applications. (a) The pH-responsive hydrogel formation from DXL homopolymerization and i-motif interlocking. Reproduced/Adapted from 10.1002/marc.202100182 with permission from Macromolecular Rapid Communications. (b) The DXL nanotube templated long conducting polymer nanonecklaces with the conductivity test. Reproduced/Adapted 10.1039/C6NR01603K with permission from The Royal Society of Chemistry. (c) DXL nanotube as a polymer stamp. Reprinted (adapted) with permission from *{ACS Nano}* 2017, 11, 1, 227–238}. Copyright {2017} American Chemical Society.

Furthermore, facilitated by the programmable self-assembly design with atomic accuracy, DNA nanotechnologies have been widely applied in nanofabrication and manufacturing, providing promising approaches to complex and functional nanostructures in electronic, semiconducting, optical and sensing applications. DXL supramolecular polymerization rendered a convenient, one-stranded method to prepare nanotubes with tunable diameter and size and relatively low price. In 2016, novel long conducting polymer nanonecklaces with a “beads-on-a-string” morphology were synthesized with the DXL nanotube template (Fig. 6b).³² The nanotube was assembled with 35–40 nm in diameter and up to 60 μm in length, then an in situ oxidative polymerization of the 3-methylthiophene monomer with the presence of iron (III) chloride was performed. The polymer/DNA nanonecklaces showed good electrical properties in voltage-current response. Carneiro et al. functionalized the DXL nanotube with polyaspartic acid and proposed further applications in guided mineralization.³³ The DXL nanotube was also used to template the fabrication of polymer stamps (Fig. 6c).³⁴ DNA nanostructure are first deposited on the surface, then covered with a polymer by spin coating, which transferred the shape and morphology to the polymer film.

CONCLUSIONS AND PERSPECTIVES

Herein, we have reviewed the detailed design principle and the development process of DXL polymerization with their applications in various dimensions. With the simple two-stranded design, the DXL monomer could easily be tuned in molecular weight and morphology. Moreover, the sticky-end

interaction in the DXL monomer provides rational, selective, and direction-controllable polymerization capability which enables hierarchical self-assembly into 1D chains, 2D sheets or nanotubes, and 3D crystals. In the DXL monomer design, two main strategies have been applied. First, the palindromes for the DXL central helical domains could be designed in equal or unequal length and further endow the final structure in various curvatures. Second, the interaction could be oriented in different 3D directions by controlling the length of the overall repeating distance (the twisting of DNA duplexes). This precisely regulates the spatial arrangement of the monomers and allows for the rational design and programmable self-assembly.

In addition, the DXL nanostructures have been demonstrated in a wide variety of applications. The DXL nanotube could be applied in the skeleton of hydrogel and solid materials, while the DNA oligonucleotide could be further modified and functionalized. Furthermore, it has been applied in nanofabrication as a convenient template. In the crystals, the DXL design maintains the well-defined secondary structure with high sequence robustness, enabling the high resolution in X-ray crystallography and following determination of either guest molecule structures or the interactions between guest molecules and DNA frameworks. The DXL polymerization expands the toolbox for DNA tile-based nanostructures and leads as a versatile and highly functionalized design for the field of DNA nanotechnology with cheap, stable, and robust structures. As long as the length of each palindrome follows the design principle throughout this review, the sequence design is really flexible. This nucleic acid supramolecular polymerization strategy will further benefit applications in structural biochemistry and molecular pharmaceutical research, drug delivery, soft materials and nanofabrication.

ACKNOWLEDGMENTS

We thank NSF (CCF-2107393 and CCM1-2025187 to C.M.) for support.

REFERENCES

1. De Greef T. F. A.; Smulders M. M. J.; Wolffs M.; Schenning A. P. H. J.; Sijbesma R. P.; Meijer E. W. Supramolecular polymerization. *Chem. Rev.* **2009**, 109, 5687–5754.
2. Huang F; Scherman O. A. Supramolecular polymers. *Chem. Soc. Rev.* **2012**, 41, 5879–5880.
3. Zhang X. Supramolecular Polymer Chemistry: Past, Present, and Future. *Chinese J. Polym. Sci.* **2022**, 40, 541–542.
4. Aida T.; Meijer E. W.; Stupp S. I. Functional supramolecular polymers. *Science*. **2012**, 335, 813–817.
5. Jangizehi A.; Ahmadi M.; Seiffert S. Emergence, evidence, and effect of junction clustering in supramolecular polymer materials. *Mater. Adv.* **2021**, 2, 1425–1453.
6. Xu F.; Feringa B. L. Photoresponsive Supramolecular Polymers: From Light-controlled Small Molecules to Smart Materials. *Adv. Mater.* **2023**, 35, 2204413.
7. Seeman N. C.; Sleiman H. F. DNA nanotechnology. *Nat. Rev. Mater.* **2017**, 3, 17068.
8. Evans C. G.; Winfree E. Physical principles for DNA tile self-assembly. *Chem. Soc. Rev.* **2017**, 46, 3808–3829.
9. Pinheiro A. V.; Han D.; Shih W. M.; Yan H. Challenges and opportunities for structural DNA nanotechnology. *Nat. Nanotechnol.* **2011**, 6, 763–772.
10. Liu W.; Zhong H.; Wang R.; Seeman N. C. Crystalline two-dimensional DNA-origami arrays. *Angew. Chem. Int. Ed.* **2011**, 50, 264–267.
11. Tian C.; Zhang C.; Li X.; Li Y.; Wang G.; Mao C. Artificial, parallel, left-handed DNA helices. *J. Am. Chem. Soc.* **2012**, 134, 20273–20275.
12. Zheng M.; Li Q.; Li Q.; Paluzzi V. E.; Choi J. H.; Mao C. Engineering the Nanoscaled Morphologies of Linear DNA Homopolymers. *Macromol. Rapid Commun.* **2021**, 42, 10–13.
13. Mao D.; Paluzzi V. E.; Zhang C.; Mao C. DNA conformational equilibrium enables continuous changing of curvatures. *Nanoscale*. **2022**, 15, 470–475.
14. Liu W.; Zhong H.; Wang R.; Seeman N. C. Crystalline two-dimensional DNA-origami arrays. *Angew. Chem. Int. Ed.* **2011**, 50, 264–267.
15. Yin P.; Hariadi R. F.; Sahu S.; Choi H. M. T.; Sung H. P.; LaBean T. H.; Reif J.H. Programming DNA tube circumferences. *Science*. **2008**, 321, 824–826.
16. Afshan N.; Zheng H.; Xiao S. J. How Small DNA Minicircles Can Be Applied to Construct DNA Nanotubes? *Chinese J. Chem.* **2016**, 34, 326–330.
17. Green L. N.; Subramanian H. K. K.; Mardanlou V.; Kim J.; Hariadi R. F.; Franco E. Autonomous dynamic control of DNA nanostructure self-assembly. *Nat. Chem.* **2019**, 11, 510–520.
18. He Y.; Chen Y.; Liu H.; Ribbe A. E.; Mao C. Self-assembly of hexagonal DNA two-dimensional (2D) arrays. *J. Am. Chem. Soc.* **2005**, 127, 12202–12203.
19. Liu H.; Chen Y.; He Y.; Ribbe A. E.; Mao C. Approaching the limit: Can one DNA oligonucleotide assemble into large nanostructures? *Angew. Chem. Int. Ed.* **2006**, 45, 1942–1945.
20. Zhang C.; He Y.; Chen Y.; Ribbe A. E.; Mao C. Aligning One-Dimensional DNA Duplexes into Two-Dimensional Crystals. *J. Am. Chem. Soc.* **2007**, 129, 14134–14135.
21. Sobey T. L.; Renner S.; Simmel F. C. Assembly and melting of DNA nanotubes from single-sequence tiles. *J. Phys. Condens. Matter*. **2009**, 21, 034112.
22. Niu L.; Yang X.; Zhou J.; Mao C.; Liang H.; Liang D. Mechanism of DNA assembly as revealed by energy barriers. *Chem. Commun.* **2015**, 51, 7717–7720.

23. Zhang C.; Zhao J.; Lu B.; Seeman N. C.; Sha R.; Noinaj N.; Mao C. Engineering DNA Crystals toward Studying DNA-Guest Molecule Interactions. *J. Am. Chem. Soc.* **2023**, 145, 4853–4859.
24. Seeman N. C. Nucleic Acid Junctions and Lattices. *J. Theor. Biol.* **1982**, 99, 237-247.
25. Paukstelis P. J.; Seeman N. C. 3D DNA Crystals and Nanotechnology *Crystals*. **2016**, 6, 97.
26. Hu Q.; Li H.; Wang L.; Gu H.; Fan C.; DNA Nanotechnology-Enabled Drug Delivery Systems. *Chem. Rev.* **2019**, 129, 6459–6506.
27. Zhang Y.; Tu J.; Wang D.; Zhu H.; Maity S.K.; Qu X.; Bogaert B.; Pei H.; Zhang H. Programmable and Multifunctional DNA-Based Materials for Biomedical Applications; *Adv. Mater.* **2018**, 30, 1703658.
28. Chen T.; Ren L.; Liu X.; Zhou M.; Li L.; Xu J.; Zhu X. DNA nanotechnology for cancer diagnosis and therapy; *Int. J. Mol. Sci.* **2018**, 19, 1671.
29. Ko S.; Liu H.; Chen Y.; Mao C. DNA Nanotubes as Combinatorial Vehicles for Cellular Delivery. *Biomacromolecules* **2008**, 9, 3039-3043.
30. Delebecque C. J.; Lindner A. B.; Silver P. A.; Aldaye F. A. Organization of Intracellular Reactions with Rationally Designed RNA Assemblies. *Science*. **2011**, 333, 470-474.
31. Shi J.; Zhu C.; Li Q.; Li Y.; Chen L.; Yang B.; Xu J. F.; Dong Y.; Mao C.; Liu D. Kinetically Interlocking Multiple-Units Polymerization of DNA Double Crossover and Its Application in Hydrogel Formation. *Macromol. Rapid Commun.* **2021**, 42, 2100182.
32. Chen G.; Mao C. Long conducting polymer nanonecklaces with a ‘beads-on-a-string’ morphology: DNA nanotube-template synthesis and electrical properties *Nanoscale*. **2016**, 8, 10026-10029.
33. Kim F.; Chen T.; Burgess T.; Rasie P.; Selinger T. L.; Greschner A.; Rizis G.; Carneiro K. Functionalized DNA nanostructures as scaffolds for guided mineralization. *Chem Sci.* **2019**, 10, 10537-10542.
34. Tian C.; Kim H.; Sun W.; Kim Y.; Yin P.; Liu H. DNA Nanostructures-Mediated Molecular Imprinting Lithography. *ACS Nano*. **2017**, 10, 227-238.

TOC

